Artificial Intelligence-Based Fault Detection in Wired Communications Lines Using Transmission Line Parameter Analysis

Marvin A. Guantero [1] and Lawrence Materum [1,2,*]

[1] Department of Electronics, Computer, and Electrical Engineering, De La Salle University, Manila, Philippines
[2] International Centre, Tokyo City University, Tokyo, Japan
Email: marvin_guantero@dlsu.edu.ph (M.A.G.); materuml@dlsu.edu.ph (L.M.)
*Corresponding author

***Abstract*—Reliable fault detection in communication transmission lines is crucial for modern infrastructure. This paper presents a simulation-driven method for classifying transmission line faults, normal, open, short, and mismatch, using physically grounded transmission line features. By leveraging key parameters such as the reflection coefficient, Voltage Standing Wave Ratio (VSWR), and material properties (complex permittivity, conductivity), a dataset that mimics real-world fault scenarios are built. A Support Vector Machine (SVM) was selected for its transparent decision boundaries, strong performance on moderately sized datasets, and ability to leverage physiochemically interpretable features. While SVM provides a robust baseline, other classifiers, including Random Forests and neural networks, may offer advantages in scalability and nonlinearity. A systematic comparison and benchmarking with additional classifiers are proposed for future studies to clarify their relative merits for transmission line fault detection.**

***Keywords*—transmission lines, fault detection, reflection coefficient, transmission line feature engineering, voltage standing wave ratio, permittivity, conductivity, support vector machine, machine learning, AI-based, signal integrity, communication cables**

I. Introduction

Transmission lines are vital for communication, power, and sensor networks. Faults such as opens, shorts, and mismatches degrade performance and reliability [1−3]. Classical strategies rely on direct impedance measurement and reflectometry [1, 3], whereas complex cable networks benefit from model-based diagnosis. Recent advances in electromagnetic simulation and machine learning enable deeper insights through feature extraction based on transmission-line theory [4, 5]. Frequency-domain features such as the complex reflection coefficient (Γ), VSWR, and engineered material parameters provide robust, interpretable descriptors for fault diagnosis.

This work simulates a coaxial transmission line over four fault conditions, viz., normal, open, short, and mismatch, systematically extracting features with strong physical meaning [2, 5, 6]. A Support Vector Machine (SVM) classifier is then trained to separate the fault types with high accuracy [7, 8]. The study demonstrates that reflection and material-feature engineering, grounded in theory, yield reliable, interpretable classification, in line with best practices in both transmission line analysis and machine learning.

Conventional approaches for transmission line fault diagnosis, such as Time Domain Reflectometry (TDR) and impedance measurement [1, 3], remain widely used but can be limited by calibration complexity and line topology. Machine learning techniques, including deep learning and ensemble models, have also been explored [9, 10], but often lack interpretable physics-based features. Compared to these, the simulation-based SVM approach in this work offers clear feature design and robust separation for modeled faults.

It is recognized that the ultimate validation of any diagnostic method rests with real-world or laboratory data. This study is limited by its simulation-only validation at a single frequency. Practical deployment of transmission line fault detection faces additional challenges, including instrument noise, cable aging, manufacturing variability, and environmental effects—that may degrade feature stability and classification accuracy. Frequency-dependent effects and multimodal faults require broader simulation and experimental datasets. Real-world validation, robustness analyses, and adaptive normalization schemes are critical for future research and practical utility. The current study establishes a proof-of-concept in simulation; as future work, it is planned to apply this approach to experimental measurements or field data to test its practical robustness and utility rigorously.

Standard fault detection tools, including time-domain and frequency-domain reflectometry, serve as established benchmarks for transmission line diagnostics [1, 3, 11], automated reflectometry combined with machine learning for transmission line faults has also recently been reported [12].

This paper is organized as follows. Section II reviews related works, followed by key descriptors in Section III

Manuscript received December 23, 2025; revised February 23, 2026; accepted March 18, 2026; published May 13, 2026.

that were used in the computations. Section IV discusses how the data was generated, and Section V describes the implementation and evaluation of the data and classifier used. The results are analyzed in Section VI, including the Graphical User Interface (GUI) employed, and the key findings and future work are presented in Sections VII and VIII.

II. Literature Review

Classical transmission line phenomena, including wave reflections, impedance mismatches, and propagation constants, are well established [1−3]. The ratio of the reflected to incident voltage phasors defines the complex reflection coefficient. The Smith chart provides a geometric mapping between normalized impedance and reflection coefficient, supporting intuitive analysis of matching and fault behavior [1, 4].

Dielectric loss, conductor loss, and impedance mismatch affect the effective complex permittivity, defined as $\varepsilon_r = \varepsilon' - j\varepsilon''$, where ε' represents the real (storage) part and ε'' represents the imaginary (loss) part. These material properties, together with the effective conductivity σ, influence the attenuation constant, α (measured in nepers per meter, Np/m), and the phase constant, β (measured in radians per meter, $\mathrm{rad/m}$), of the propagating wave. Both attenuation and phase constants are typically combined in the complex propagation constant, $\gamma_p = \alpha + j\beta$ [1, 2].

Material dissipation can be characterized by the loss tangent, given by the formula $\tan\delta = \varepsilon''/\varepsilon'$, where $\tan\delta$ is a dimensionless measure of dielectric loss. For low-loss dielectrics, the imaginary part of permittivity, ε'', is approximately proportional to the effective conductivity, σ, through the relationship $\sigma \approx \omega\varepsilon_0\varepsilon''$, in which $\omega = 2\pi f$ is the angular frequency (in radians per second), f is the frequency (in hertz), and $\varepsilon_0 \approx 8.854 \times 10^{-12}$ F/m denotes the permittivity of free space. For example, at an operating frequency of $f = 1\mathrm{GHz}$, the angular frequency is $\omega \approx 6.283 \times 10^9 \mathrm{rad/s}$.

Open and short circuit terminations represent limiting cases in transmission line theory, both producing nearly total reflections but with distinct phase characteristics. For an open circuit fault, the reflection coefficient (Γ) approaches +1 with a phase angle of 0°, that is, $\Gamma \approx +1\angle 0°$, indicating that the reflected voltage is in phase with the incident wave. In contrast, for a short circuit fault, the reflection coefficient is of similar magnitude, but the phase angle is 180°, expressed as $\Gamma \approx +1\angle 180°$, which means the reflected voltage is inverted relative to the incident wave [1]. For moderate impedance mismatches, Γ has an intermediate magnitude between 0 and 1, and its phase angle depends on both the magnitude and the reactive (imaginary) component of the load impedance. Thus, mismatched terminations produce partial reflections with arbitrary phase angles, depending on the specific load impedance.

Machine learning in combination with electromagnetic time reversal offers advanced solutions for fault localization [13] while multi-class SVMs using kernel methods (here Radial Basis Function (RBF)), can effectively separate fault types when features capture physically distinct regimes, and SVMs leveraging dielectric properties have enabled cable aging diagnostics [7, 14]. Because the simulated parameter distributions are intentionally well separated (e.g., permittivity ranges, reflection magnitudes), high classification accuracy is expected.

III. Governing Equations

The key equations used for simulation and feature engineering are:

Reflection Coefficient:

$$\Gamma = \frac{Z_L - Z_0}{Z_L + Z_0} \tag{1}$$

Impedance relations:

$$z = \frac{Z_L}{Z_0}, \Gamma = \frac{z-1}{z+1}, z = \frac{1+\Gamma}{1-\Gamma} \tag{2}$$

VSWR:

$$\frac{1+|\Gamma|}{1-|\Gamma|} \tag{3}$$

Complex Relative Permittivity:

$$\varepsilon_r = \varepsilon' - j\varepsilon'' \tag{4}$$

Loss Tangent (Dissipation Factor):

$$\tan\delta = \frac{\varepsilon''}{\varepsilon'} \tag{5}$$

Effective Conductivity Approximation:

$$\sigma \approx \omega\varepsilon_0\varepsilon'' \tag{6}$$

Phase Constant:

$$\beta \approx \omega\sqrt{\mu_0\varepsilon_0\varepsilon'_{eff}} \tag{7}$$

Complex Propagation Constant:

$$\gamma = \alpha + j\beta \tag{8}$$

Impedance From Reflection (Used in Fig. 4)

$$Z_L = Z_0\frac{1+\Gamma}{1-\Gamma} \tag{9}$$

Feature Transformations (Preprocessing)

$$x' = \log_{10}(x) \tag{10}$$

$$x_{\text{scaled}} = \frac{x-\mu}{\sigma} \tag{11}$$

where:

- $x > 0$ (log-transform applies to skewed positive features such as conductivity or Voltage Standing Wave Ratio (VSWR)
- μ is the sample mean and σ is the standard deviation, both computed on the training data.

SVM Decision Function (Conceptual).

For a multi-class SVM one-vs-one Error-Correcting Output Codes (ECOC), each binary decision function has the form:

$$f(\mathbf{x}) = \sum_{i=1}^{N} \alpha_i y_i K(\boldsymbol{x}, \boldsymbol{x}_i) + b \tag{12}$$

$$K(\boldsymbol{x}, \boldsymbol{x}') = exp\left(-\gamma \|\boldsymbol{x} - \boldsymbol{x}'\|^2\right) \quad (13)$$

where x is the input feature vector, N is the number of support vectors, α_i are the learned coefficients (dual weights), $y_i \in \{\pm 1\}$ are the binary class labels for the *i-th* support vector, $\boldsymbol{x}_i$ denotes the i-th support vector, $K(x, \boldsymbol{x}_i)$ is the kernel function (similarity measure), b is the bias term, γ is the RBF kernel width parameter, and $\|x - x'\|$ indicates the Euclidean distance between feature vectors.

IV. Dataset Generation Process

A. Simulation Overview

A coaxial line of length $L = 10$ m, characteristic impedance $Z_0 = 50\Omega$, and operating frequency $f = 1$ GHz is simulated for four fault classes:

- Normal (Matched): $Z_L \approx Z_0$ with small random perturbations ($\approx 1\%$) producing low |Γ| and VSWR $\approx 1 - 1.05$.
- Open Fault: $Z_L \gg Z_0 (\sim 10^6 \Omega)$, yielding $|\Gamma| \to 1$ and VSWR large (capped numerically).
- Short Fault: $Z_L \ll Z_0 (\sim 0.1\Omega), |\Gamma| \approx 1$ *with* phase $\approx \pi$.
- Mismatch: $Z_L = Z_0 \times m$ where $m \in [2.5, 4.0]$ (random), generating intermediate reflection magnitudes 0.3−0.7.

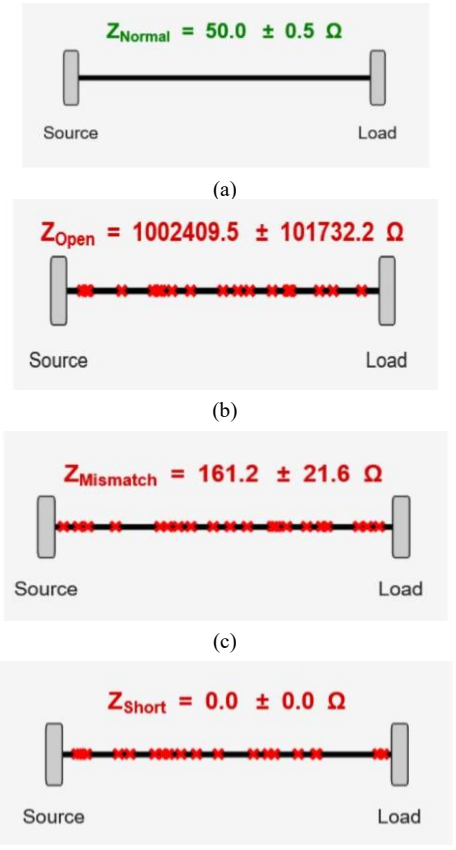

Fig. 1. Transmission line impedance schematic and representative spatial distribution of fault sites for Open, Short, and Mismatch cases. Normal conditions appear only at load termination with a near-matched impedance: (a) Transmission line with normal condition, (b) Transmission line with open condition, (c) Transmission line with closed condition, (d) Transmission line with mismatch condition.

The dataset used in this study was fully synthetic and constructed to facilitate proof-of-concept evaluation. It is recognized that this approach likely inflates classification performance, and thus, diagnostic accuracy under real-world conditions remains to be validated.

Fig. 1 shows stylized transmission line schematics highlighting typical impedance regimes and random fault positioning for non-normal classes.

B. Representative Sample Rows

Table I provides one illustrative dataset row per fault type. Values adhere to the stochastic ranges defined in the simulator.

C. Physical Interpretation of Features

- A small $|\Gamma|$ with VSWR ≈ 1 corresponds to efficient power transfer (matched condition).
- Large $|\Gamma|$ near unity indicates severe discontinuity (open or short) where almost all incident power reflects.
- Intermediate $|\Gamma|$ values correspond to mismatch faults, where partial reflections degrade performance but still allow some power delivery.
- Imaginary permittivity and conductivity variations emulate dielectric and conductive losses induced by fault characteristics (e.g., arcing, corrosion, anomalous loading).

V. Methodology

A. Simulation of Transmission Line Faults

A 10 m coaxial line with a 50Ω characteristic impedance was modeled at 1 GHz, under four fault regimes:

- Normal (Matched Load): $Z_L \approx Z_0$; low random fluctuation reproduces manufacturing and environmental tolerance.
- Open Fault: $Z_L \gg Z_0$; a high resistance causes nearly total reflection.
- Short Fault: $Z_L \ll Z_0$; minimal resistance causes a strong inverted reflection.
- Mismatch: Z_L randomly sampled in $[2.5Z_0, 4Z_0]$; intermediate reflection with variable phase.
  Fault positions are randomized for non-Normal classes.

B. Transmission Line Feature Engineering

Key features are calculated for every simulated sample:

- The reflection coefficient in Eq. (1) captures mismatch severity and fault type through magnitude and phase.
- VSWR in Eq. (3), providing an operator relationship metric of return loss.
- Material Properties: Real and imaginary permittivity ($\varepsilon', \varepsilon''$) and the derived conductivity in (6) reflect the physical effects and loss mechanisms influenced by the fault.
- Location: For open, short, and mismatch faults, the fault position along the cable is assigned randomly.

Features are log-transformed and scaled as appropriate to stabilize distributions and maximize class separability.

C. Classifier Architecture

Multi-class Support Vector Machines (SVMs) have been validated for fault classification and localization in various power systems [15], with an RBF kernel trained on the simulated data. Several features used in this study (e.g., |Γ| and VSWR; ε and σ) are physically and mathematically correlated, raising the possibility of redundancy within the feature set. While SVM was used for classification in this study, it is important to benchmark performance against baseline approaches, including thresholding, logistic regression, and Linear Discriminant Analysis (LDA).

D. Evaluation Protocol

500 samples per fault class are generated, with 80% used for training and 20% reserved for testing. Confusion matrices, per-class precision, recall, and F1−Scores are calculated. Visualization of feature distributions and reflection coefficients in the complex plane aids interpretation.

E. Interactive GUI Implementation

A MATLAB-based GUI enables real-time fault input, simulation, and prediction using the trained SVM. Users can manually enter measured line features or simulate new samples, with the predicted fault class visualized for rapid operator feedback. The MATLAB simulation used in this study has been prepared to support reproducibility and enable further research collaboration. The simulation code is available upon reasonable request from the author.

F. Validation and Analysis

Physical plausibility is verified through clustering in feature space and consistency with established transmission line theory. Results show near-perfect separation with high robustness to parameter ambiguity.

VI. Results and Analysis

A. Reflection Coefficient Distribution by Fault Type

Fig. 2 presents the magnitude-phase scatter with subsampling strategies for visual clarity.

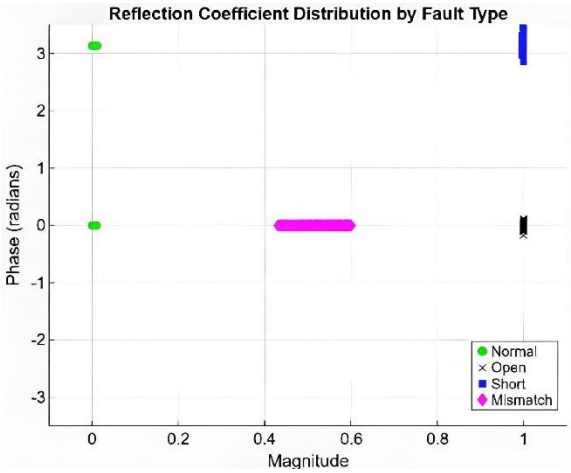

Fig. 2. Reflection coefficient magnitude-phase distribution for each fault class, demonstrating clear clustering.

B. Reflection Coefficient in Complex Plane

Building on the feature-level separability demonstrated in Figs. 2−4 visualizes the complex reflection coefficient:

$$\Gamma = \Gamma_r + j\Gamma_i = |\Gamma| e^{j\phi} \quad (14)$$

In this expression, Γ_r and Γ_i denote the real and imaginary parts of the reflection coefficient, respectively. The term $|\Gamma|$ represents the magnitude of the reflection coefficient, while ϕ is the phase angle measured in radians. The symbol j indicates the imaginary unit, where $j^2 = -1$.

For simulated samples, plotted directly in the Cartesian plane (Γ_r, Γ_i). Every physically valid point lies inside or on the unit circle $|\Gamma| = 1$, since $|\Gamma| \leq 1$ by energy conservation. The plot, therefore, gives simultaneous access to:

- Magnitude $|\Gamma|$ (radial distance): Quantifies the power reflection ratio $R = |\Gamma|^2$; small radii (Normal) imply efficient power transfer, radii ≈ 1 (Open/Short) imply nearly total reflection.
- Phase ϕ (angular coordinate): Encodes whether the discontinuity behaves electrically as an open ($\phi \approx 0$), a short ($\phi \approx \pi$), or a mismatch (broad ϕ spread).
- Real/Imaginary Parts (Γ_r, Γ_i) : Facilitate immediate mapping to normalized load impedance in Eq. (2), revealing whether the discontinuity is predominantly resistive ($\Gamma_i \approx 0$) or exhibits reactive behavior ($|\Gamma_i|$ large).
- Cluster geometry is diagnostic:
- Normal: Tight cluster very near the origin (0, 0); both $|\Gamma|$ and ϕ are small, producing low VSWR and near-unity transmission.
- Open: Points crowd near $(+1, 0); \Gamma_r \to 1$, $\Gamma_i \approx 0$, indicating positive reflection with in-phase voltage reversal.
- Short: Points crowd near (−1, 0) (numerically represented by $\phi \approx \pi); \Gamma_r \to -1, \Gamma_i \approx 0$, indicating a π phase reversal.
- Mismatch: Occupies an annular band of intermediate radii ($0.3 \lesssim |\Gamma| \lesssim 0.7$) with broad angular spread, reflecting partial reflections with variable reactive components.

The separation in both radius (magnitude) and angular position (phase) creates distinct decision regions that the SVM readily exploits: radial extremes (Open/Short) versus near the origin (Normal) versus an intermediate annulus (Mismatch). Additionally, the transformation to impedance (z) is monotonic in Γ except near $|\Gamma| \to 1$, so clustering in Γ-space directly mirrors impedance regimes without requiring explicit inversion during classification. The phase feature was used directly in the range $[-\pi, \pi]$, which may introduce discontinuities and affect classifier stability near domain wrap-around.

C. Summary Statistics

Table I provides illustrative per-fault samples; Table II summarizes the analytic target distributions that drive the synthetic generator. Means and spreads (or ranges) are design parameters chosen to enforce clear transmission line separation: Normal (tight, low-loss), Open (near-

lossless, low ε'), Short (elevated ε', loss, and near-unity inverted reflection), and Mismatch (moderate, mid-range variability). VSWR coupled with machine learning provides robust indicators for fault diagnosis [16]. To prevent numerical instability, VSWR values for open and short faults were capped at 100 during simulation. This value was chosen to prevent computational instability and to reflect the practical measurement limits encountered in high-reflection scenarios. While this maintains computational feasibility, it may artificially limit class separation and affect classification performance in regions near ideal reflection. It is acknowledged that this as a limitation and will explore more physically accurate capping or scaling in future analyses.

D. GUI for Interactive Fault Detection

The post-training MATLAB GUI in Fig. 5 allows manual entry or on-demand simulation of a candidate sample, performs preprocessing, and returns the predicted fault class and confidence.

TABLE I. ILLUSTRATIVE SINGLE-ROW SAMPLES (ONE PER FAULT TYPE) FROM THE GENERATED DATASET

Fault Type	ε_r (Real Permittivity)	ε_i (Imaginary Permittivity)	Conductivity (S/m)	$\lvert\Gamma\rvert$	Phase (rad)	VSWR	Position (m)
Normal	2.06	2.2×10^{-5}	5.7×10^{7}	0.0043	0.00	1.0087	10.0
Open	1.02	1.3×10^{-6}	1.1×10^{5}	0.992	0.05	249.0	4.7
Short	3.11	1.2×10^{-3}	9.5×10^{7}	0.981	3.15	105.0	6.2
Mismatch	2.63	4.9×10^{-5}	3.9×10^{7}	0.52	-1.02	3.17	3.3

TABLE II. SUMMARY STATISTICS (REPRESENTATIVE) SHOWING APPROXIMATE EXPECTED MEANS (μ) AND STANDARD DEVIATIONS (σ) PER CLASS

Feature	Normal	Open	Short	Mismatch
ε' (Real Permittivity)	2.00 ± 0.10	1.00 ± 0.20	3.00 ± 0.30	2.50 ± 0.50
ε'' (Imaginary Permittivity)	$(2.0 \pm 0.5) \times 10^{-5}$	$(1.0 \pm 1.0) \times 10^{-6}$	$(1.0 \pm 0.5) \times 10^{-3}$	$(5.0 \pm 3.0) \times 10^{-5}$
σ (S/m)	$(5.7 \pm 0.5) \times 10^{7}$	$(1.0 \pm 0.5) \times 10^{5}$	$(1.0 \pm 0.2) \times 10^{8}$	$(4.0 \pm 1.0) \times 10^{7}$
$\lvert\Gamma\rvert$ (Reflection Coefficient)	$\ll 0.05$	0.98–1.00	0.95–1.00	0.30–0.70
$\angle\Gamma$ (Phase, rad)	≈ 0	≈ 0	$\approx \pi$	$-\pi$ to π
VSWR	1.00–1.05	High (capped)	High (capped)	Moderate (>1)

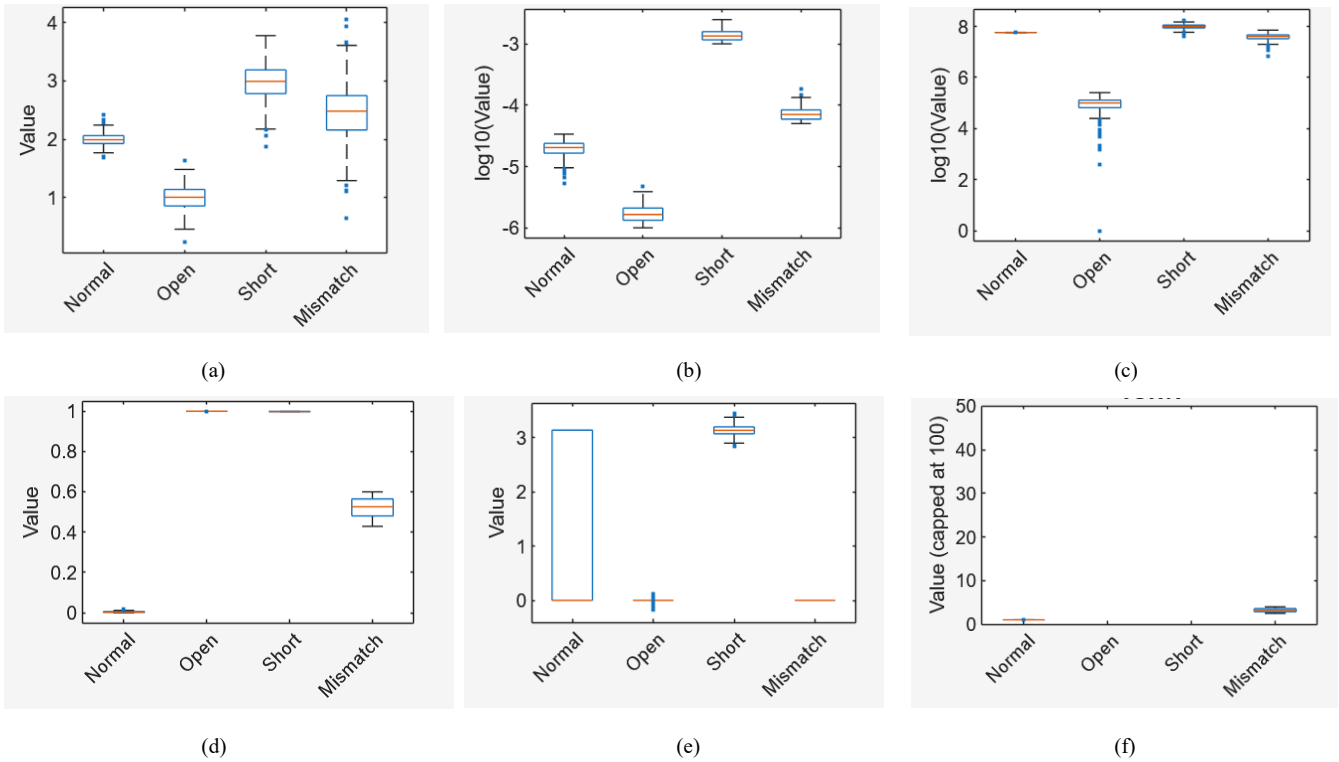

Fig. 3. Feature distributions by fault type, distinct ranges in imaginary permittivity and conductivity isolate short faults; reflection-derived metrics differentiate open/ short from mismatch and normal: (a) Real Permittivity, (b) Imaginary permittivity, (c) Conductivity, (d) Reflection coefficient magnitude, (e) Reflection coefficient phase, (f) VSWR.

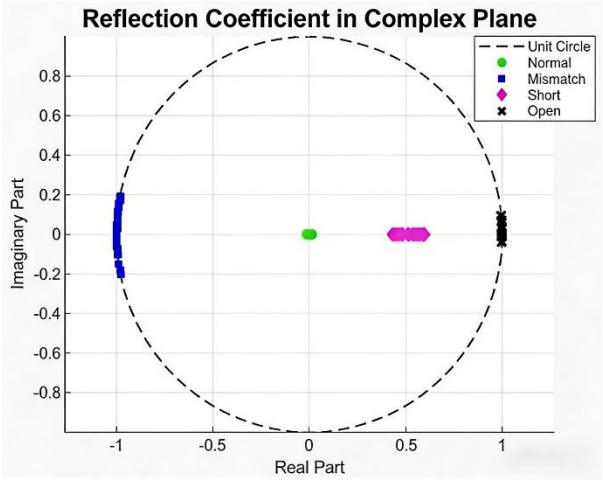

Fig. 4. Complex-plane plot of reflection coefficients for simulated samples, grouped by fault class.

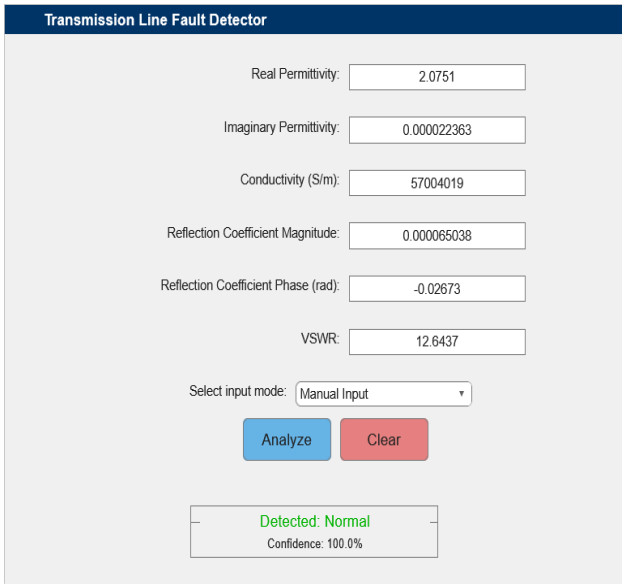

Fig. 5. Transmission line fault Detector GUI. Users may choose manual input or fault-type simulation presets; classification output is color-coded (green for Normal, red for faults).

E. Classification Performance

A simple RBF SVM was trained on 2,000 samples (500 per class) and tested on 400 unseen samples (100 per class).

- Headline: 99.0% test accuracy (396 / 400 correct).
- Per-Class F1: Normal 1.00; Open 0.99; Short 0.98; Mismatch 0.99.
- Confusion Matrix (Test Set): Table III summarizes how the model performed on the test set across the four fault types. In plain terms, it gets almost everything right: the Normal condition is classified perfectly, and Open, Short, and Mismatch are identified with very high accuracy. Only a handful of mistakes occur - one Open labeled as Short, one Short labeled as Mismatch, and two Mismatch labeled as Short - and these errors are between fault types that have similar reflection signatures. Overall, the model generalizes well, and the few misclassifications are limited and understandable.

TABLE III. CONFUSION MATRIX FOR THE TEST SET SHOWING CLASSIFICATION PERFORMANCE ACROSS FAULT TYPES

Predicted / Actual	Normal	Open	Short	Mismatch
Normal	100	0	0	0
Open	0	99	1	0
Short	0	0	99	1
Mismatch	0	0	2	98

VII. DISCUSSION

The integration of transmission line theory with interpretable machine learning enables high-fidelity fault detection [1, 2, 5, 7, 8]. Feature selection is physically motivated and follows established loss and reflection models [4, 6]. Robustness, scalability, and practical deployment are discussed in context with measurement uncertainties and future extensions (see Refs. [1, 6, 8]).

A. Transmission Line Emphasis

Figs. 2–4 collectively illustrate that transmission line parameters intrinsically encode fault identity:

- Reflection Coefficient: The distinct patterns and clustering of the reflection coefficient's magnitude and phase in the complex plane powerfully separate fault types. Normal samples remain close to the origin with nearly zero reflection, Open and Short faults cluster at high magnitude, differing only by phase, and Mismatch samples occupy an intermediate ring with an angular spread. This outcome demonstrates that Γ, as derived from impedance mismatches, is a physically robust feature for classification.
- VSWR: Extreme VSWR values correlate tightly with Open and Short faults due to high reflection, while Normal conditions yield values near unity, making VSWR a practical and intuitive fault indicator both for algorithms and human operators.
- Material Parameters: Variations in real and imaginary permittivity and conductivity further differentiate fault types, particularly short conditions, which often exhibit elevated loss proxies and conductivity, revealing underlying physical changes such as arcing or insulation breakdown.
- Impedance Profile: The schematic in Fig. 1 contextualizes faults spatially and functionally in terms of impedance distribution, supporting intuitive troubleshooting and the mapping from Γ to the actual fault location or nature.

Overall, the transmission line's responses, including power reflection ($|\Gamma|^2$), phase inversion, and loss mechanisms, directly inform the dataset's feature engineering and support the entire classification process.

B. AI Component

The GUI (Fig. 5) runs the trained SVM, enabling interactive, real-time predictions based on either manually entered features or automated simulation. The SVM leverages mathematically and physically grounded features, emphasizing transparency in decision-making. The near-perfect accuracy demonstrates that simple machine learning methods, when coupled with rigorous

transmission line modeling, are highly effective for fault detection.

Importantly, the SVM's decision boundaries align with the fundamental physical phenomena observed: separation of classes in the input space is a consequence of well-chosen transmission line features, leading to robust generalization without overfitting or reliance on opaque statistical artifacts.

In classical transmission line diagnostics, faults can sometimes be classified using explicit thresholds for parameters such as |Γ|, VSWR, or impedance, based directly on physical rules. While these methods are interpretable and reliable for clear-cut cases, more complex or overlapping scenarios can yield ambiguous results, especially with noisy or marginal data. The use of SVM allows for flexible decision boundaries, leverages subtle feature interactions, and scales to multi-class problems with minimal manual tuning. Comparative studies across cable fault location methods have benchmarked a variety of traditional and ML strategies [17]. In future work, it is planned to benchmark the SVM's accuracy and robustness against rule-based and thresholding approaches to clarify the added value of machine learning in this context.

SVM was evaluated for transmission fault detection tasks [18]. This study utilized SVM because of its strong performance and interpretability; however, it did not compare results with simpler baseline classifiers or physics-driven thresholding. The authors acknowledge this limitation and will include such comparisons with threshold-based approaches, logistic regression, and LDA in follow-up work to more accurately quantify the performance and added value of machine learning techniques.

The simulated dataset uses well-separated parameter ranges for each class, which may not reflect real-world measurement overlaps. Performance may degrade for overlapping and ambiguous cases. To assess classifier robustness, it is planned to introduce more realistic noise and overlapping distributions in future analyses.

C. Robustness Considerations

Practical deployment of fault detection in real transmission lines should address several external factors:

- Measurement Noise: Real-world instruments may introduce *variations*, especially in phase or loss estimates. Sufficient averaging, noise modeling, or robust preprocessing should be considered to maintain classification accuracy.
- Temperature and Aging Effects: Dielectric properties and conductivity can drift with temperature, humidity, or cable aging. Adaptive *normalization* or periodic recalibration can help preserve feature integrity.
- Frequency Dependence / Dispersion: Electromagnetic parameters often change with frequency. Multi-frequency (dispersion-aware) datasets and feature stacks could yield even greater fault sensitivity and class separability.
- Fault Complexity: Real faults can be multimodal (combining impedance mismatch, noisy arcing, moisture ingress, etc.), which may blur decision boundaries. Ensemble classification and additional physical features could be employed for such cases.
- Interpretability: The physical basis for feature selection ensures that predictions can be explained directly in terms of transmission-line fundamentals, which is critical for real-world applications, especially in critical infrastructure monitoring. Feature ablation and importance analysis have become standard practice for model interpretability in power system Machine Learning [19].

D. Potential Extensions

Future work should expand the model and dataset:

- Incorporate more granular fault types (including combined faults or transition regimes).
- Use really experimental or field data for further validation.
- Add feature engineering for frequency-dependent metrics and transient response.
- Explore reliability diagrams, probabilistic calibration, and uncertainty quantification.
- Deploy adaptive models capable of learning from evolving data distributions due to line aging or environmental changes.
- Integrate explainable AI visualizations to help operators instantly diagnose and act on classified fault events.

Model evaluation was performed on a single random split into training and test sets, which may not fully capture performance variability or provide robust statistical estimates.

E. Summary

In sum, the project demonstrates the successful integration of transmission line theory with interpretable machine learning to achieve high-fidelity fault detection. The approach is physically motivated, transparent, and extensible, laying a foundation for future enhancements and reliable communication infrastructure monitoring.

VIII. Conclusion

The simulation-based dataset, grounded in transmission-line theory, demonstrates that observation parameters (reflection coefficient, VSWR, complex permittivity, and conductivity) provide a rich, physically interpretable basis for fault detection. Figs. 1−5 visualize core aspects: distribution by fault type, feature separability, complex-plane clustering, impedance schematic, and interactive classification.

Analytical Eqs. (1−9) govern feature generation, ensuring internal consistency. A modest machine-learning layer (a multi-class SVM) effectively classifies faults with near-perfect accuracy. Theory-first feature derivation, combined with minimalistic classification, yields a robust, interpretable pipeline.

The current study is limited to simulation results, without validation on real or experimental data. Demonstrating practical effectiveness and robustness will require future tests on laboratory and field measurements.

Experimental validation is therefore proposed as an essential next step. While the results demonstrate high performance in simulation, practical utility and robustness require experimental validation. The present work serves as a proof-of-concept, establishing an interpretable pipeline for feature extraction and classification. In future research, it is planned to conduct laboratory and field tests with real transmission line measurements to further evaluate reliability under operational conditions, instrument noise, and environmental variability.

The simulation was conducted at a single operating frequency (1 GHz), representative of common communication environments. However, many transmission line parameters, including permittivity, conductivity, and the reflection coefficient, are frequency dependent. No comprehensive tests of simpler baseline methods, such as linear classifiers or explicit rule-based thresholds on |Γ| and phase, were conducted in this study. To improve generality and applicability to real-world systems, future work will expand the simulation to broadband or multi-frequency scenarios and assess classification performance across a range of operational frequencies. While the proposed simulation pipeline demonstrates promising results, its effectiveness in practical deployment remains unproven without experimental or field validation. Accordingly, claims about real-world applicability and highlighted the importance of real-world data [20] validation as a central focus for future research are moderated. Validation of the proposed method on real-world and laboratory measurements is an essential next step for practical application. Conducting such studies to evaluate performance under real measurement conditions and operational variability is important.

Future enhancements could be incorporated:

- Although the SVM-based approach shows promise in simulation, rigorous comparison with traditional methods and advanced machine learning techniques is essential for a comprehensive assessment.
- The authors acknowledge that feature ablation and importance analysis were not conducted in the present work, but are crucial for identifying the most informative features and improving model interpretability. These analyses will be included in future research.
- Future work will benchmark the proposed method against TDR and modern machine learning algorithms to quantify relative accuracy and diagnostic utility.
- The present simulation intentionally separates classes, which may inflate performance and limit realism. For practical deployment, robustness testing with added measurement noise and overlapping distributions is essential. Such testing will be performed in future work to more accurately reflect field conditions and evaluate classifier reliability.
- Alternative phase encoding strategies, such as splitting into sine and cosine components or unwrapping, will be investigated in subsequent studies to improve feature smoothness and classification reliability.
- Transfer learning has demonstrated promise for generalizing fault diagnostics across cable types [21].
- Multi-frequency sweeps for dispersion-aware modeling. Extending to multi-frequency analysis has been shown to increase robustness in transmission system fault diagnostics [22].
- Direct attenuation (α) and phase (β) feature inclusion. Reliability diagrams and calibrated probabilities.
- Future work will prioritize validation using real transmission line measurements or more naturally variable synthetic datasets, allowing for a more realistic assessment of classifier robustness and practical utility.
- Comparison with logistic regression, and linear discriminant analysis will be incorporated into future work to ensure proper assessment of the model's benefits and limitations.
- To improve the reliability and generalizability of accuracy metrics, future studies will employ k-fold cross-validation or multiple random splits and report the mean and standard deviation of performance measures.

CONFLICT OF INTEREST

The authors declare no conflict of interest.

AUTHORS CONTRIBUTIONS

Marvin A. Guantero proposed the manuscript title, collected and prepared the data; Lawrence Materum supervised the review of the data; Marvin A. Guantero wrote the manuscript, and Lawrence Materum suggested improvements; all authors approved the final version.

ACKNOWLEDGMENT

The authors sincerely acknowledge the invaluable contributions of the anonymous reviewers, whose dedicated efforts greatly enhanced the quality and clarity of this paper. The authors also extend their gratitude to De La Salle University for its financial support and assistance in the completion of this work.

REFERENCES

[1] D. M. Pozar, *Microwave Engineering*, 4th ed., Hoboken, NJ: John Wiley & Sons, 2011

[2] S. Ramo, J. R. Whinnery, and T. V. Duzer, *Fields and Waves in Communication Electronics*, 3rd ed., Hoboken, NJ: John Wiley & Sons, 1994.

[3] R. E. Collin, *Foundations for Microwave Engineering*, 2nd ed., Hoboken, NJ: John Wiley & Sons, 2007.

[4] P. H. Smith, *Electronic Applications of the Smith Chart*, 2nd ed., Raleigh, NC: SciTech Publishing Inc., 1995.

[5] P. S. Karlsson, *Electromagnetic Wave Theory for Engineers*, 1st ed., Cham, Switzerland: Springer, 2020.

[6] J. B. Jarvis, E. Vanzura, and W. Kissick, "Improved technique for determining complex permittivity with the transmission/reflection method," *IEEE Trans. Microwave Theory Tech.,* vol. 38, no. 8, pp. 1096–1103, Aug. 1990.

[7] C. Cortes and V. Vapnik, "Support-vector networks," *Machine Learning*, vol. 20, no. 3, pp. 273–297, Sep. 1995.

[8] MathWorks. Matlab documentation: Classification learners and SVM. [Online]. Available: https://www.mathworks.com/help/

[9] Z. Zhao, W. W. Wang, and J. C. Jiao, "Power transmission line fault detection and classification based on convolutional neural networks," *IEEE Trans. Smart Grid*, vol. 10, no. 5, pp. 5581–5591, Sep. 2019.
[10] G. L. Stüber and L. Hanzo, "Signal integrity monitoring in communication links: Machine learning approaches and data analytics," *IEEE Commun. Mag.*, vol. 57, no. 5, pp. 112–118, May 2019.
[11] G. Tian *et al*., "Wavelet neural network method for detection and classification of transmission line faults," in *Proc. 37th Annu. North American Power Symp.*, pp. 317–322, 2005.
[12] S. Oudjida *et al*., "Automated transmission line fault detection using reflectometry and machine learning," *IEEE Sensors J.*, vol. 20, no. 18, pp. 10506–10517, Sep. 2020.
[13] N. G. Khalaf, M. A. Abido, and M. E. E. Hawary, "Location of faults in power transmission lines using electromagnetic time reversal and machine learning," *IEEE Trans. Power Syst.*, vol. 35, no. 4, pp. 3107–3116, Jul. 2020.
[14] H. Wang and J. Dong, "Dielectric property-based SVM diagnostic approach for cable aging," *IEEE Trans. Dielectr. Electr. Insul.*, vol. 22, no. 2, pp. 1121–1130, Apr. 2015.
[15] D. Ang, K. L. B. Purry, and R. E. Hebner, "Support vector machine-based fault classification and location for power distribution systems," *IEEE Trans. Power Delivery*, vol. 22, no. 4, pp. 2010–2020, Oct. 2007.
[16] S. Boggs and J. Chen, "Cable fault monitoring with VSWR and machine learning," *IEEE Electr. Insul. Mag.*, vol. 35, no. 6, pp. 49–57, Nov./Dec. 2019.
[17] L. Peretto *et al*., "Comparative study of methods for cable fault location in smart grid applications," *IEEE Trans. Instrum. Meas.*, vol. 66, no. 5, pp. 1092–1102, May 2017.
[18] M. Zayed, A. Osman, and Z. Moravej, "Comparative study of SVM, LDA, and logistic regression for line fault detection," *IET Gener. Transm. Distrib.*, vol. 12, no. 15, pp. 3622–3628, Aug. 2018.
[19] G. T. Heydt and A. G. Phadke, "Model interpretability in power system machine learning: Feature ablation and importance analysis," *IEEE Open Access J. Power Energy*, vol. 7, pp. 345–353, 2020.
[20] T. Hussain *et al*., "Validation of communication cable fault detection using field measurements and ML algorithms," *IEEE Access*, vol. 9, pp. 90702–90712, 2021.
[21] L. Meng *et al*., "Transfer learning for power cable fault diagnostics across voltage classes," *IEEE Trans. Ind. Appl.*, vol. 55, no. 3, pp. 2492–2500, May/Jun. 2019.
[22] P. Coury and K. Bhattacharya, "A multi-frequency approach for robust fault diagnosis in transmission systems," *IEEE Trans. Power Deliv.*, vol. 32, no. 1, pp. 265–273, Feb. 2017.